

On the incorporation of nickel and cobalt into MoS₂-edge structures

Mingyong Sun^a, Alan E. Nelson^{a,*}, John Adjaye^b

^a University of Alberta, Department of Chemical and Materials Engineering, Edmonton, Alberta, Canada T6G 2G6

^b Syncrude Canada Ltd., Edmonton Research Centre, Edmonton, Alberta, Canada T6N 1H4

Received 11 March 2004; revised 3 May 2004; accepted 5 May 2004

Available online 5 June 2004

Abstract

The present study investigates the details of MoS₂-edge surfaces modified with different loadings of nickel and cobalt using density-functional theory (DFT) under generalized gradient approximation (GGA) considering the effect of sulfidation conditions. Although this has been the subject of previous studies, a comprehensive understanding of the promoted edge surfaces is not complete. Under typical sulfidation conditions, nickel prefers to incorporate into the metal edge and cobalt the S-edge of MoS₂. On a partially promoted metal edge surface, sulfur atoms bond to the surface on top of the molybdenum atoms and the promoter atoms tend to be uncovered. The adsorbed sulfur atoms atop of molybdenum atoms and the neighboring uncovered promoter atoms provide pairs of base (or nucleophile) and acid sites for surface catalytic reactions.

© 2004 Elsevier Inc. All rights reserved.

Keywords: Molybdenum sulfide; Nickel-promoted molybdenum sulfide; Cobalt-promoted molybdenum sulfide; Hydrotreating; Density-functional theory

1. Introduction

Nickel- and cobalt-promoted MoS₂ catalysts are widely used in hydrotreating processes to remove sulfur and nitrogen-containing compounds from various oil fractions. The active sites on MoS₂-based catalysts are located on the edge surfaces of the MoS₂ layered structure, and the incorporation of nickel or cobalt into the MoS₂ structure significantly increases the activity of the catalyst [1,2]. Among many models for interpreting the synergetic effect between cobalt (or nickel) and molybdenum, the CoMoS theory proposed by Topsøe et al. is generally accepted [3], although this model has been challenged by the remote control and contact theory [4], and the support effects theory [5].

The determination of MoS₂-edge structures and energetics has also been the subject of several theoretical investigations, and these have been recently reviewed elsewhere [6]. Although several groups have studied the energetics and geometric configurations of promoted MoS₂-edge surfaces [7–11], a comprehensive understanding of the promoted edge surfaces is not complete. Some of these stud-

ies focused on the promoted S-edge [7], and others on the promoted metal-edge [8,10]. Most of the studies emphasized Co-promoted catalysts rather than Ni-promoted edge surfaces [7–10]. Schweiger et al. studied both cobalt- and nickel-promoted S-edge and metal-edge MoS₂ catalysts using triangular cluster models; however, no energetic results were reported for partially promoted edge surfaces [11].

By means of scanning tunneling microscopy (STM), Lauritsen et al. obtained atomic-scale images of a CoMoS cluster on a gold surface, showing that the cobalt atoms locate at the shorter S-edges ($\bar{1}010$ surface) of a truncated hexagonal MoS₂ cluster [12]. However, computational investigations using different theoretical models have suggested that the S-edge ($\bar{1}010$ surface) [7,9], Mo-edge ($10\bar{1}0$ surface) [8], and bulk structure [13] are the preferred locations for cobalt. In these studies, the effect of sulfidation conditions on the relative stabilities of different structures with different sulfur coverages on the surface was not considered. Schweiger et al. calculated the surface energies of the S-edge and Mo-edge separately for unpromoted [14] and fully promoted catalysts [11]. By comparing the surface energies of different promoted edge structures of triangular cluster models, they discovered that cobalt favours the S-edge and nickel the metal-edge under typical sulfidation conditions.

* Corresponding author. Fax: (780) 492-2881.

E-mail address: alan.nelson@ualberta.ca (A.E. Nelson).

The objective of this study is to provide additional clarification on the local structures of CoMoS and NiMoS catalysts with different promoter loadings using density-functional theory (DFT). The present approach uses periodic slab models and considers the effect of temperature and $p_{\text{H}_2\text{S}}/p_{\text{H}_2}$ ratio on the relative stability of the edge structures. The S-edge and metal-edge are studied as partially and fully promoted by nickel and cobalt, and the effect of sulfidation conditions is considered for the relative stability of the edge structures. In order to provide a solid foundation for the discussions of nickel and cobalt incorporation into MoS₂ edge structures, the energetics and structures of unpromoted MoS₂ are examined using the same model as used for the promoted catalysts. New surface configurations are identified as the most stable structures under sulfidation conditions using this approach, and the potential implications to hydrotreating catalysts are discussed.

2. Methods

2.1. DFT calculations

The DFT calculations were performed using Material Studio DMol³ from Accelrys (version 2.2) [15]. The electronic wavefunctions are expanded in numerical atomic basis sets defined on an atomic-centered spherical-polar mesh. The double-numerical plus *d* functions (DND) all electron basis set is used for all the calculations. The DND basis set includes one numerical function for each occupied atomic orbital and a second set of functions for valence atomic orbitals, plus a polarization *d* function on all atoms. Each basis function is restricted to within a cutoff radius of 4.5 Å, allowing for efficient calculations without loss of accuracy. The exchange-correlation energy is approximated by the Becke exchange functional [16] in conjunction with the Perdew–Wang correlation functional [17] in all calculations (GGA-BP). The Kohn–Sham equations [18] are solved by a SCF (self-consistent field) procedure. Techniques of direct inversion in an iterative subspace (DIIS) [19] with a size value of 6, thermal smearing [20], and a range of 0.005 Ha are applied to accelerate convergence. The calculation quality control settings are medium for all geometry optimizations, and the optimization convergence thresholds for energy change, maximum force, and maximum displacement between optimization cycles are 0.00002 Ha, 0.004 Ha/Å, and 0.005 Å, respectively. Based on the convergence test for *k*-point sampling, the *k*-point set of (2 × 1 × 1) was used for calculations of the Ni- and Co-promoted and unpromoted MoS₂ slab models. Spin polarization was applied to all calculations for the systems containing magnetic elements (nickel or cobalt).

2.2. Molybdenum-based catalyst models

Fig. 1 shows the periodic slab models including four S–Mo–S rows in the *y* direction, two S–Mo–S units in the

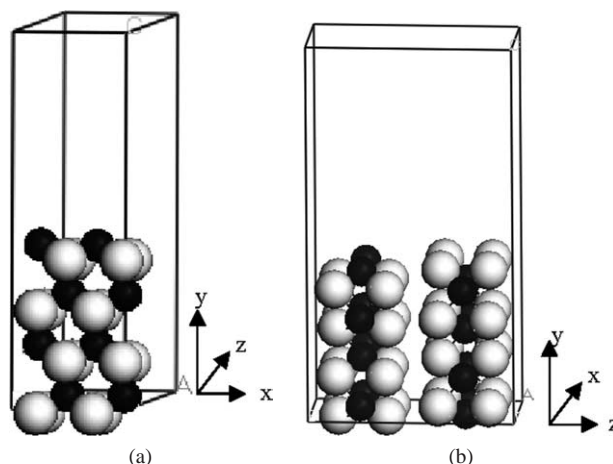


Fig. 1. MoS₂ models, including (a) the single layer model, and (b) the two-layer model. Each model comprises four molybdenum rows (4-Mo). Black balls, molybdenum atoms; light grey, sulfur.

x direction, and one layer (a) or two layers (b) in the *z* direction. In order to clarify the effects of the catalyst model on calculation results, a series of calculations using different sizes of MoS₂ model catalysts was performed by varying the periodicity in the *x* direction (two and four), the number of rows in the *y* direction (two to six), and the number of layers in the *z* direction (one and two). The different models resulted in a similar general trend of the change in relative energy with varying sulfur coverage on the Mo edge of MoS₂. Furthermore, the changes in relative energies by enlarging the model from two to four units in the *x* direction, four rows to six rows in the *y* direction, and one layer to two layers in the *z* direction were insignificant. As a result of the comparisons, the single-layer four-rows (2 × 4) model (Fig. 1a) is primarily used in calculating the relative energetics of different surface structures of MoS₂ catalysts. During the geometry optimization, the atoms in the two inner S–Mo–S rows are fixed as in the bulk structure and other atoms at both edge surfaces are relaxed. Considering that the incorporation of promoter atoms at the edge surfaces may lead to surface reorganization, a double-sized supercell including four metal atoms in the *x* direction (4 × 4) is also used to examine the stable structures of partially promoted surfaces, which allows more freedom in geometry optimization.

2.3. Thermodynamic calculations

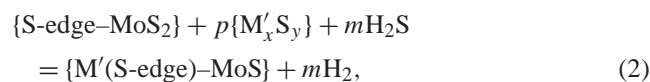
Relative energies of the surfaces with different sulfur coverages are calculated according to similar methods as described in literature [7,8,10,21–23]. The free energy change for adding *n* sulfur atoms on the reference surface at temperature *T*, $p_{\text{H}_2\text{S}}$, and p_{H_2} can be calculated by

$$\Delta G = \Delta E_0 + n\Delta G_{T_{\text{corr}}}^0 - nRT \ln \frac{p_{\text{H}_2\text{S}}}{p_{\text{H}_2}}, \quad (1)$$

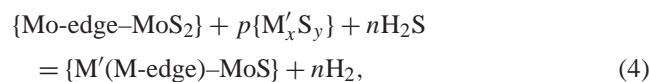
where ΔE_0 is the standard energy change at 0 K, and $\Delta G_{T_{\text{corr}}}^0$ the temperature correction for free energy change

from 0 to T K. $\Delta G_{T_{\text{corr}}}^0$ varies from 0.31 eV at 575 K to 0.40 eV at 675 K.

In order to determine which edge is energetically preferred for cobalt and nickel substituting edge molybdenum atoms, the energetics for the incorporation of promoter sulfides into the S-edge and into the Mo-edge are calculated as follows:



$$\begin{aligned} \Delta G_{\text{S-edge}} = E_{0,M'(\text{S-edge})\text{MoS}} - E_{0,\text{S-edge-MoS}_2} \\ - pE_{M'_xS_y} + m(E_{0,\text{H}_2} - E_{0,\text{H}_2\text{S}}) \\ + m\Delta G_{T_{\text{corr}}}^0 - mRT \ln \frac{p_{\text{H}_2\text{S}}}{p_{\text{H}_2}}, \end{aligned} \quad (3)$$



$$\begin{aligned} \Delta G_{\text{Mo-edge}} = E_{0,M'(\text{M-edge})\text{MoS}} - E_{0,\text{Mo-edge-MoS}_2} \\ - pE_{M'_xS_y} + n(E_{0,\text{H}_2} - E_{0,\text{H}_2\text{S}}) \\ + n\Delta G_{T_{\text{corr}}}^0 - nRT \ln \frac{p_{\text{H}_2\text{S}}}{p_{\text{H}_2}}. \end{aligned} \quad (5)$$

$\{\text{S-edge-MoS}_2\}$ and $\{\text{Mo-edge-MoS}_2\}$ represent unpromoted MoS₂ catalyst models exposing the stable S-edge and Mo-edge, respectively, $\{M'_xS_y\}$ the promoter sulfide, $\{M'(\text{S-edge})\text{-MoS}\}$ and $\{M'(\text{M-edge})\text{-MoS}\}$ the promoted catalyst with promoter at the S-edge and at the metal-edge, respectively. $\Delta G_{\text{S-edge}}$ and $\Delta G_{\text{Mo-edge}}$ are defined as the *synergic energies* for incorporating promoters into the S-edge and Mo-edge, respectively. The *relative synergic energy* between incorporations of one type promoter into the S-edge and Mo-edge can be calculated by subtracting Eq. (5) from (3), which is used to determine the edge preference for cobalt and nickel incorporation into MoS₂-edge structures.

3. Results and discussion

3.1. Energetics and geometric structures of edge surfaces for MoS₂ and Co(Ni)MoS catalysts

The relative energies (ΔE_0) of the unpromoted and promoted MoS₂ as a function of sulfur coverage for the metal edges are presented in Fig. 2 and for S-edges in Fig. 3. Adsorption of one, two, or four sulfur atoms on the Mo-edge surface of the supercell gives 25, 50, and 100% sulfur coverages, respectively [7,8,21]. Figs. 4, 5, and 6 plot the relative free energies (ΔG) of different edge surfaces of unpromoted MoS₂, Ni(Co)-promoted MoS₂ with 50% or 100% of edge molybdenum atoms being substituted by nickel (or cobalt) as functions of the $p_{\text{H}_2\text{S}}/p_{\text{H}_2}$ ratio at 650 K. For each edge, the 50% sulfur coverage surface is taken as reference.

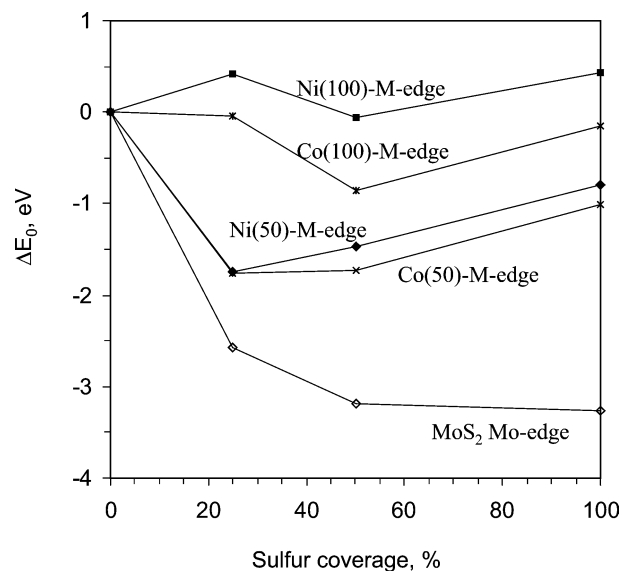


Fig. 2. Relative energies of MoS₂ promoted by cobalt or nickel as function of sulfur coverage on the metal-edge, with the bare surfaces being used as references. M'(50)-M-edge and M'(100)-M-edge refer to promoted catalyst with 50% and 100% of molybdenum atoms on the Mo-edge substituted by promoter atoms M'(Co or Ni).

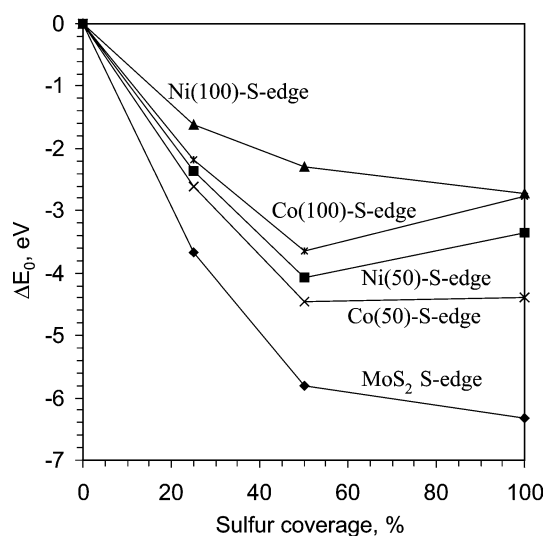


Fig. 3. Relative energies of MoS₂ promoted by cobalt or nickel as function of sulfur coverage on the S-edge, with the bare surfaces being used as references. M'(50)-S-edge and M'(100)-S-edge refer to promoted catalyst with 50% and 100% of molybdenum atoms on the S-edge substituted by promoter atoms M'(Co or Ni).

For unpromoted MoS₂, at very high $p_{\text{H}_2\text{S}}/p_{\text{H}_2}$ ratios fully sulfided Mo-edge and S-edge surfaces are stable. The required $p_{\text{H}_2\text{S}}/p_{\text{H}_2}$ ratio for a fully sulfided S-edge is lower than that for a fully sulfided Mo-edge. It is possible to remove more sulfur atoms to create vacancies from the Mo-edge of 50% sulfur coverage by decreasing the $p_{\text{H}_2\text{S}}/p_{\text{H}_2}$ ratio to very low levels (Fig. 4a); however, it is not from the S-edge of 50% sulfur coverage. The excellent agreement obtained in energetics and surface structure for unpromoted MoS₂ confirms the results obtained by other groups using

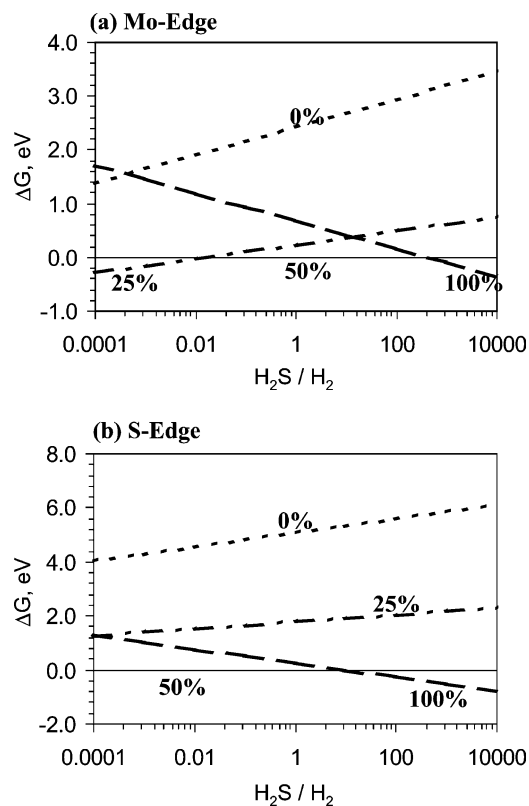


Fig. 4. Relative energies of MoS₂ as function of $p_{\text{H}_2\text{S}}/p_{\text{H}_2}$ ratios at 650 K, (a) Mo-edge, (b) S-edge. Each line is labeled by the corresponding sulfur coverage on the edge surface, with 50% sulfur coverage taken as reference (solid line).

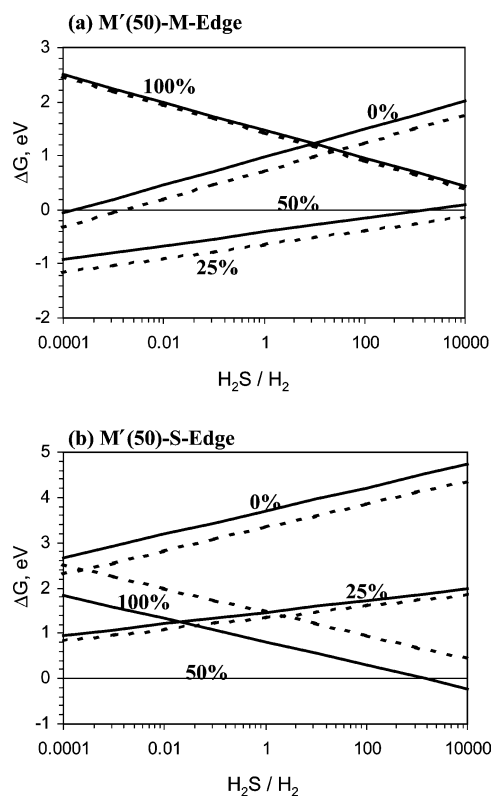


Fig. 5. Relative free energies of M'(50)-M-edge (a), and M'(50)-S-edge (b) as a function of $p_{\text{H}_2\text{S}}/p_{\text{H}_2}$ ratios at 650 K. Dash lines, M' = Ni; solid lines, M' = Co. Each line is labeled by the corresponding sulfur coverage on the edge surface, with 50% sulfur coverage taken as reference.

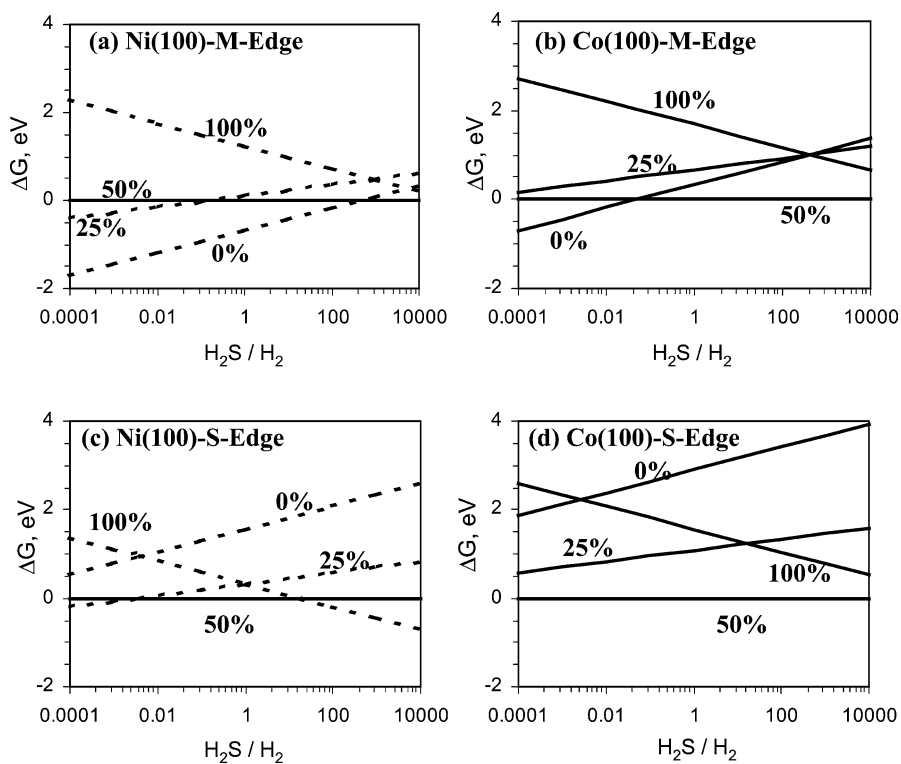


Fig. 6. Relative free energies of M'(100)-M-edge (a, b), and M'(100)-S-edge (c, d) as a function of $p_{\text{H}_2\text{S}}/p_{\text{H}_2}$ ratios at 650 K. Dash lines, M' = Ni; solid lines, M' = Co. Each line is labeled by the corresponding sulfur coverage on the edge surface, with 50% sulfur coverage taken as reference.

different models and software packages [7,21,22,24]. More importantly, it establishes a solid foundation for the following investigation of the structure and properties of promoted catalysts.


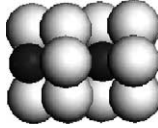
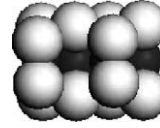


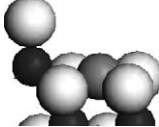

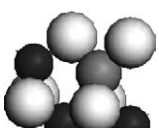
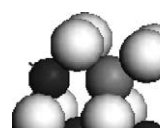
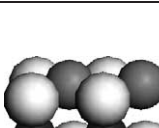
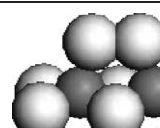


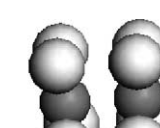
For the CoMoS and NiMoS catalysts, the cobalt and nickel atoms are located at edge surfaces by substituting the edge molybdenum atoms [8,12]. Substitution of one molybdenum atom of every two by a promoter atom ($M' = \text{Co}$ or Ni) on the S-edge or Mo-edge generates an edge structure with 50% molybdenum atoms substituted by promoter atoms (cobalt or nickel), $M'(50)\text{-S-edge}$ or $M'(50)\text{-M-edge}$, respectively. When promoter atoms substitute all of the edge molybdenum atoms, a fully promoted surface, $M'(100)\text{-S-edge}$ or $M'(100)\text{-M-edge}$, is generated.

On the $M'(50)\text{-M-edge}$, the 25% sulfur coverage is the most stable for both Ni- and Co-promoted surfaces (Fig. 5a), in which the sulfur atoms bond to the surface on top of the molybdenum atoms (structure f in Table 1). If an additional sulfur atom is added to the partially promoted metal-edge surface of 25% sulfur coverage, this sulfur atom prefers to join the preadsorbed sulfur atom and form a S–S dimer directly on top of the molybdenum atom (structure g in Table 1). Such a configuration is stable at very high $p_{\text{H}_2\text{S}}/p_{\text{H}_2}$ ratios for the Co-promoted metal edge (Fig. 5a). To obtain the 100% sulfur coverage, a pair of sulfur atoms is placed on top of each surface metal atom. The sulfur atoms that are originally located directly on top of nickel atoms tend to move away from the nickel and combine with the sulfur atoms on the molybdenum to form dimers, which are not stable under sulfidation conditions. For the S-edge substitution, the 50% sulfur coverage surface (structure h) is the most stable for most $p_{\text{H}_2\text{S}}/p_{\text{H}_2}$ ratios.

New geometrical configurations of sulfur atoms on the edge surfaces emerge from the partially (50%) promoted MoS_2 model catalysts. On the metal edge, $M'(50)\text{-M-edge}$, when one sulfur atom is placed on the Ni(50)-M-edge surface of the supercell, the sulfur atom prefers to bond solely to the molybdenum atom directly atop. The bridging location for sulfur on the partially Ni-promoted Mo-edge is unstable. When the sulfur atom is placed bridging molybdenum and nickel atoms, it migrates to the top of the molybdenum atom during geometrical optimization. For Co(50)-M-edge, there is a local minimum in which the sulfur atom bridges the molybdenum and the cobalt atoms. However, the configuration with sulfur directly atop has a lower energy by 0.7 eV. Therefore, there is a similar trend for the nickel(50)- and cobalt(50)-promoted metal edge: the sulfur atoms prefer to bond to molybdenum atoms atop rather than to promoter atoms or to bridge the molybdenum and the promoter atoms.

Byskov et al. [7], Raybaud et al. [8], and Travert et al. [10] also studied the configuration of sulfur atoms on the partially Co-substituted Mo-edge, and none of them identified the configuration with sulfur atoms on the top of the remaining molybdenum atoms as the most stable structure. Instead, they considered the sulfur atoms at bridging locations between cobalt and molybdenum atoms as the stable structure,

Table 1
The optimized surface structures of unpromoted and promoted Mo-edge and S-edge with different sulfur coverages

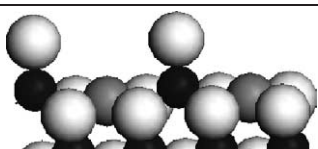
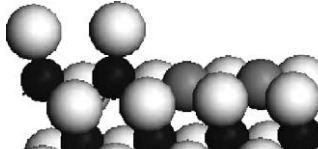
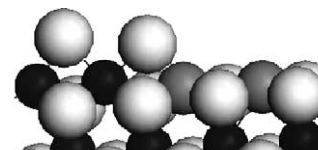
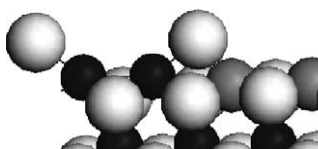

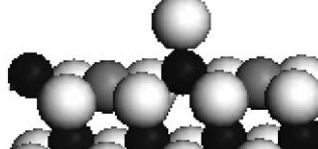
MoS_2 Mo-edge			
(S%)	a (25%)	b (50%)	c (100%)
MoS_2 S-edge			
(S%)	d (50%)	e (100%)	
$M'(50)\text{-M-edge}$			
(S%)	f (25%)	g (50%)	
$M'(50)\text{-S-edge}$			
(S%)	h (50%)	i (100%)	
$M'(100)\text{-M-edge}$			
(S%)	j (25%)	k (50%)	
$M'(100)\text{-S-edge}$			
(S%)	l (25%)	m (50%)	n (100%)

Black balls, molybdenum atoms; dark grey, promoter atoms; light grey, sulfur; S%, sulfur coverage; $M'(50)\text{-M-edge}$ and $M'(100)\text{-M-edge}$, M' stands for promoter (Co or Ni), 50 and 100 for 50% and 100% of edge molybdenum atoms are substituted by promoter atoms, respectively, M-edge for promoter on the metal-edge; $M'(50)\text{-S-edge}$ and $M'(100)\text{-S-edge}$, promoter M' (Co or Ni) on the S-edge.

which according to the present study is only a local minimum.

In order to further confirm that the new geometrical configuration is not due to using a smaller supercell including two surface metal atoms, a double-sized model was used to further optimize the partially promoted metal-edge surface. The optimized surface structure of the double-sized supercell (4×4) is given in Table 2 (structure o), which is the same as the one obtained using the smaller one (2×4). The total energy of the optimized structure in the (4×4) supercell is only 0.01 eV lower than twice that in the (2×4) supercell. This confirms that the sulfur atop edge geometrical

Table 2
The optimized surface structures and relative energies of Ni(50)–M-edges in a (4×4) supercell

Surface configurations	ΔE (eV)
	0
	0.05
	0.12
	–
	0.26
	1.73

Black balls, molybdenum atoms; dark grey, promoter atoms; light grey, sulfur. H_2 and H_2S are used as references for the atom balance in calculating the relative energies of structures s and t.

try is the most stable configuration on the partially promoted metal-edge surface, and that the (2×4) model is sufficient to represent the partially promoted metal edge. The energy required to remove a sulfur atom from structure o is only 0.01 eV less than that required to remove the sulfur atom from structure f (Table 1), which indicates that the interaction between the two adsorbed sulfur atoms in structure o is insignificant.

Additional configurations using the larger supercell, in which the two nickel atoms are not separated by molybdenum atoms (structures p, q, r, s in Table 2), were also studied. On such a partially promoted metal surface, every two molybdenum atoms on the Mo-edge are substituted by two nickel atoms alternatively, termed $(2 + 2) \times 4$ model. If the structure o is taken as energetic reference, structure p is only slightly higher in total energy. If the two sulfur

atoms are located bridging molybdenum and nickel atoms as shown by structure r, after optimization the sulfur atoms will relocate to the top of molybdenum atoms to yield the configuration of structure p. These results clearly indicate that the sulfur atoms tend to be adsorbed on the top of molybdenum atoms and leave the promoter atoms uncovered.

The (4×4) supercell model also facilitates the calculation of the relative energy for a lower sulfur coverage surface, considering only one sulfur atom being adsorbed on the four-metal surface. The energetically favored location for the sulfur atom is to bridge the two molybdenum atoms on the $(2 + 2) \times 4$ surface, structure s in Table 2, and directly on top of one molybdenum atom when molybdenum atoms are separated by nickel atoms, structure t in Table 2. The energies for structure s and structure t are 0.26 and 1.73 eV relative to structure o, taking hydrogen and hydrogen sulfide as references. At low p_{H_2S}/p_{H_2} ratios, structure s is more stable than structure p.

The previous results clearly indicate that on a partially promoted metal edge, the nickel atoms are uncovered while the molybdenum atoms are covered by sulfur atoms. When molybdenum atoms are separated by nickel atoms the sulfur atoms are adsorbed directly atop; otherwise, the sulfur atoms prefer to bridge two neighboring molybdenum atoms.

Substitution of all the edge surface molybdenum atoms by cobalt or nickel atoms further reduces the bonding of sulfur atoms on the edge surfaces. The fully Ni-promoted metal edge surface, Ni(100)–M-edge, tends to be uncovered by sulfur atoms (structure j in Table 1), except for very high p_{H_2S}/p_{H_2} ratios (> 500) where sulfur atoms bond to the surface in the form of a weak S–S dimer (structure k in Table 1). The optimized geometrical configurations on the Co(100)–M-edge are similar to that on the Ni(100)–M-edge as shown in Table 1; however, the bonding of sulfur on the cobalt surface is stronger than that on the nickel surface. The corresponding p_{H_2S}/p_{H_2} ratio shifts from 500 for Ni(100)–M-edge to 0.05 for Co(100)–M-edge, above which the 50% sulfur coverage surface is more stable than the bare surface (Fig. 6b). On the fully promoted S-edge, the sulfur coverage can vary from 25% at very low p_{H_2S}/p_{H_2} ratios (< 0.004), 50% at middle p_{H_2S}/p_{H_2} ratios (0.004 to 20), to 100% at high p_{H_2S}/p_{H_2} ratios (> 20) (Fig. 6c) for the Ni(100)–S-edge surface. For the Co(100)–S-edge surface, the 50% sulfur coverage is preferred for all p_{H_2S}/p_{H_2} ratios shown in Fig. 6d. The optimized stable surface geometric configurations for different sulfur coverages on the fully promoted S-edge are presented in Table 1 (structures l, m, n).

On the bare surface of Ni(100)–M-edge each nickel atom is coordinated to four sulfur atoms. The addition of one sulfur atom on such a surface is an endothermic process. If an additional sulfur atom is added, the two sulfur atoms tend to dimerize on the surface (structure k in Table 1). The formation of the S–S dimer on the surface stabilizes the sulfur atoms on the surface (Fig. 2). When two additional sulfur atoms are placed on the Ni(100)–M-edge surface of 50% sulfur coverage, they have a strong tendency to move

away from the surface, and the 100% sulfur coverage on the Ni(100)–M-edge surface is not stable relative to 50% sulfur coverage. A similar trend exists for the Co(100)–M-edge. The stable configurations for the fully promoted metal-edge with 50% sulfur coverage (structure k in Table 1) were missed in previous studies [8,11].

The fully sulfided S-edge has the lowest energy for the Ni(100)–S-edge, while the 50% sulfided S-edge has the lowest energy for the Co(100)–S-edge (Fig. 2). On the Ni(100)–S-edge surface, the sulfur atoms migrate to the top of the nickel atoms from the bridging positions between nickel atoms, where they are originally placed prior to optimization. A similar configuration was reported by Schweiger et al. for the fully sulfided Ni(100)–S-edge [11]. Cobalt atoms on the fully sulfided Co(100)–S-edge do not have such a strong preference to the planar configuration. The difference in energetics between configurations with sulfur atoms at the bridging positions and that with sulfur atoms on top of cobalt atoms is less than 0.1 eV, and both are unstable compared to 50% sulfur coverage with sulfur atoms at bridging positions on the metal plane. With 50% sulfur coverage on the fully promoted S-edge, the sulfur atoms prefer bridging locations for both nickel- and cobalt-promoted surfaces.

3.2. Preferred location for the promoter atoms

The synergic energies of the promoted S-edge relative to corresponding promoted metal-edge planes are presented in Fig. 7 for nickel (Fig. 7a) and cobalt (Fig. 7b). The changes in the slopes of $(\Delta G_{S\text{-edge}} - \Delta G_{\text{Mo-edge}})$ vs $p_{\text{H}_2\text{S}}/p_{\text{H}_2}$ plots are due to changes in reference structures for the unpromoted edges and the changes in the promoted edge structures as functions of $p_{\text{H}_2\text{S}}/p_{\text{H}_2}$ ratios in calculating $\Delta G_{S\text{-edge}}$ and $\Delta G_{\text{Mo-edge}}$ values. Figs. 4, 5, and 6 present the $p_{\text{H}_2\text{S}}/p_{\text{H}_2}$ ranges in which the unpromoted and promoted structures are stable with corresponding sulfur coverages on the surfaces.

For the 50% nickel-promoted edge surfaces (dash line, Fig. 7a), $(\Delta G_{S\text{-edge}} - \Delta G_{\text{Mo-edge}})$ is positive at very low $p_{\text{H}_2\text{S}}/p_{\text{H}_2}$ ratios (< 0.2), which indicates that the S-edge is less favourable than the Mo-edge for nickel incorporation. At higher $p_{\text{H}_2\text{S}}/p_{\text{H}_2}$ ratios, $(\Delta G_{S\text{-edge}} - \Delta G_{\text{Mo-edge}})$ becomes negative, which indicates the S-edge is more favourable. The $p_{\text{H}_2\text{S}}/p_{\text{H}_2}$ ratio during the sulfidation of

hydrotreating catalysts is typically less than 0.2. Thus, the incorporation of nickel into the Mo-edge is preferred over the S-edge for 50% nickel-promoted catalysts at typical sulfidation conditions. The difference in the synergic energy between S-edge and Mo-edge incorporation, however, is only about 0.14 eV at low $p_{\text{H}_2\text{S}}/p_{\text{H}_2}$ ratios. This suggests that both structures are possible under normal sulfidation conditions, with the ratio of Boltzmann populations of Ni(50)–S-edge to Ni(50)–M-edge about 0.082 [10].

For the 100% nickel-promoted edge surfaces (solid line, Fig. 7a), $(\Delta G_{S\text{-edge}} - \Delta G_{\text{Mo-edge}})$ is positive over a broad range of $p_{\text{H}_2\text{S}}/p_{\text{H}_2}$ ratios (< 60). At very low $p_{\text{H}_2\text{S}}/p_{\text{H}_2}$ ratios (< 0.01), the value of $(\Delta G_{S\text{-edge}} - \Delta G_{\text{Mo-edge}})$ is larger than 0.9 eV, indicating the Mo-edge is energetically preferred over the S-edge for nickel incorporation. The ratio of Boltzmann populations of Ni(100)–S-edge to Ni(100)–M-edge is about 10^{-7} ; therefore, it is almost impossible to obtain a fully nickel-promoted S-edge at very low $p_{\text{H}_2\text{S}}/p_{\text{H}_2}$ ratios. The incorporation of nickel into the S-edge is only favoured at very high $p_{\text{H}_2\text{S}}/p_{\text{H}_2}$ ratios.

For the 50% cobalt-promoted catalyst (dash line, Fig. 7b) at low $p_{\text{H}_2\text{S}}/p_{\text{H}_2}$ ratios (< 0.02), $(\Delta G_{S\text{-edge}} - \Delta G_{\text{Mo-edge}})$ is -0.08 eV; therefore, both the cobalt-promoted metal edge and S-edge are present with significant populations (approx 20 vs 80%). At higher $p_{\text{H}_2\text{S}}/p_{\text{H}_2}$ ratios, $(\Delta G_{S\text{-edge}} - \Delta G_{\text{Mo-edge}})$ ranges from -0.5 to -0.1 eV and the relative population of the cobalt-promoted metal edge varies accordingly from 0.01 to 20%. For the 100% cobalt-promoted edge surfaces (solid line, Fig. 7b), the preference of the promoter atoms for the S-edge is even stronger. The $(\Delta G_{S\text{-edge}} - \Delta G_{\text{Mo-edge}})$ reaches the most negative value, -0.55 eV at $p_{\text{H}_2\text{S}}/p_{\text{H}_2}$ ratios between 0.05 and 10, which indicates that cobalt has a strong preference to the S-edge at this range of $p_{\text{H}_2\text{S}}/p_{\text{H}_2}$ ratios.

This result confirms the STM observation that cobalt is located at the S-edge covered by sulfur atoms at bridge positions by Lauritsen et al. [12]. For Ni-promoted MoS₂ model catalysts, one may obtain different edge structures at normal sulfidation conditions, since the metal edge is preferred at low $p_{\text{H}_2\text{S}}/p_{\text{H}_2}$ ratios (Fig. 7a).

This result also confirms the general conclusion obtained by Schweiger et al., who used triangular cluster models and

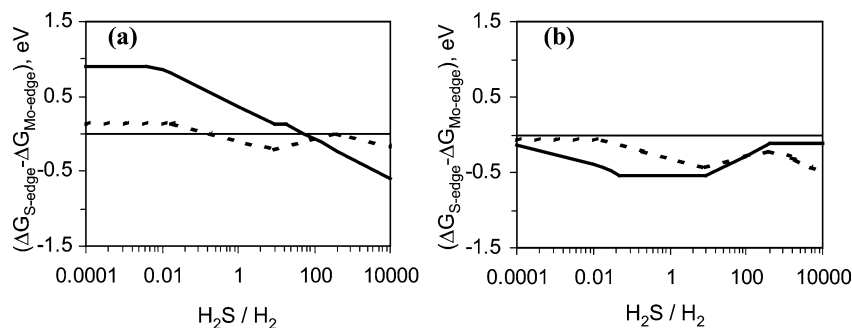


Fig. 7. Relative synergic energies of M'(50)–S-edge (dash line), and M'(100)–S-edge (solid line) as a function of $p_{\text{H}_2\text{S}}/p_{\text{H}_2}$ ratios at 650 K, M'(50)–M-edge and M'(100)–M-edge being used as references, respectively. (a) M' = Ni, (b) M' = Co.

the surface energies of the promoted S-edge and metal edge to discuss the edge preference for promoters [11]. In the calculation of the surface energy of the promoted S-edge or metal edge, the bulk MoS₂ was taken as the reference [11]. The synergic energy, however, uses the unpromoted Mo-edge and S-edge as references for incorporating promoters into the metal edge and S-edge, respectively (Section 2.3). It has been shown that the surface energy of the unpromoted S-edge is higher than that of the unpromoted Mo-edge under sulfidation conditions, both relative to bulk MoS₂ [14]. Using the relative surface energy to discuss the promoter edge preference neglects the difference in the surface energy between the unpromoted S-edge and Mo-edge. Therefore, the promoted S-edge would be underestimated relative to the promoted Mo-edge in discussing the edge preference of the promoters by using the surface energy instead of the synergic energy. Calculations using the surface energy and the *synergic energy* would obtain the same general conclusions about the preferred locations of promoters when the difference in the relative energy between the unpromoted Mo-edge and S-edge is smaller than the difference in the synergetic energy between the metal-edge and S-edge incorporations, otherwise they would not.

3.3. Implications of the stable edge structures of promoted MoS₂ catalysts in catalysis

The results obtained from this study have direct implications for HDN and HDS reactions. The mechanism of C–N bond cleavage in the HDN of aliphatic nitrogen-containing molecules has been suggested to be Hofmann-type elimination or nucleophilic substitution [25–29]. Both of these mechanisms require a pair of sites: an acid site to react with the nitrogen molecule through the nitrogen atom, making the amine group ready to leave from the molecule; and a basic site to abstract the β -hydrogen in the elimination mechanism, or a nucleophile to attack the α -carbon in the nucleophilic substitution mechanism.

On the partially Ni-substituted Mo-edge (structure f), which is stable under sulfidation conditions, the uncovered promoter atoms can accommodate the nitrogen-containing molecules as adsorption sites (Lewis acid sites) and the neighboring sulfur atoms can be the basic sites or the nucleophile. Rota et al. have proposed a similar model in discussing stereochemistry of the HDN of cyclohexylamines over NiMo catalysts [30]. It should be emphasized that such an active site configuration can only exist on the partially promoted metal edge. The salient structural features for unpromoted MoS₂ preclude the existence of these required neighboring basic and acidic sites on the unpromoted Mo-edge.

While nickel prefers the metal-edge, cobalt prefers the S-edge under the sulfidation conditions. On the Co-promoted S-edge, sulfur atoms bridge the metal atoms similar to the unpromoted S-edge. The incorporation of promoters decreases the sulfur–metal bonding, which means that the ac-

tivity of sulfur atoms on the S-edge increases with the loading of promoters. Ni-promoted catalysts are superior to Co-promoted catalysts for hydrogenation and HDN, while the opposite is true for HDS [1,2]. Comparing the edge surface structures of Ni-promoted and Co-promoted molybdenum sulfide catalysts will provide fundamental insights into why these two types of catalysts behave differently. The absence of bare metal sites on the Co-promoted edge surface may explain the low activity of Co-promoted catalysts in hydrogenation and HDN. The high HDS activities of Co-promoted catalysts indicate that the Co-promoted S-edge has the required active site configuration for HDS reactions, in which the sulfur is located at bridging positions. Further computational studies are required to understand how sulfur-containing compounds are activated on the sulfur-covered cobalt-promoted S-edge.

The above discussions are based on the equilibrium surface structure that are stable at sulfidation conditions. Under typical hydrotreating reaction conditions, the competition of reacting molecules for active sites must be considered. However, additional studies are also required to understand the competitive adsorption of various molecules on the edge surfaces to develop a detailed understanding of HDN and HDS reaction mechanisms.

4. Conclusions

The sulfidation conditions not only affect the equilibrium sulfur coverage on the edge surfaces of unpromoted MoS₂ catalysts, but also affect the edge preferences of promoters. Under normal sulfidation conditions, nickel prefers the metal-edge and cobalt the S-edge. The difference in edge preference between nickel and cobalt, which leads to different surface structures and properties, is suggested to be partly responsible for the difference in catalytic performance in hydrodesulfurization and hydrodenitrogenation reactions. On a partially promoted Mo-edge surface, the existence of the adsorbed sulfur atoms on top of molybdenum atoms and the neighboring uncovered promoter sites provide pairing base (or nucleophile) and acid sites for surface catalytic reactions. It is possible to preferentially substitute the molybdenum atoms on either the S- or the Mo-edge to different extents by insightful manipulation of the catalyst preparation and sulfidation procedures.

Acknowledgments

This work is supported by Syncrude Canada Ltd. and the Natural Sciences and Engineering Research Council (NSERC) under Grant CRDPJ 261129-01.

References

- [1] R. Prins, V.H.J. de Beer, G.A. Somorjai, *Catal. Rev.-Sci. Eng.* 31 (1989) 1.
- [2] H. Topsøe, B.S. Clausen, F.E. Massoth, in: *Hydrotreating Catalysis, Science and Technology*, vol. 11, Springer, Berlin, 1996.
- [3] H. Topsøe, B.S. Clausen, R. Candia, C. Wivel, S. Morup, *J. Catal.* 68 (1984) 433.
- [4] P. Grange, X. Vanhaeren, *Catal. Today* 36 (1997) 375.
- [5] J.C. Duchet, E.M. van Oers, V.H.J. de Beer, R. Prins, *J. Catal.* 80 (1983) 336.
- [6] M. Sun, J. Adjaye, A.E. Nelson, *Appl. Catal. A* 263 (2004) 131.
- [7] L.S. Byskov, J.K. Nørskov, B.S. Clausen, H. Topsøe, *J. Catal.* 187 (1999) 109.
- [8] P. Raybaud, J. Hafner, G. Kresse, S. Kasztelan, H. Toulhoat, *J. Catal.* 190 (2000) 128.
- [9] L.S. Byskov, J.K. Nørskov, B.S. Clausen, H. Topsøe, *Catal. Lett.* 64 (2000) 95.
- [10] A. Travert, H. Nakamura, R.A. van Santen, S. Cristol, J.F. Paul, E. Payen, *J. Am. Chem. Soc.* 124 (2002) 7084.
- [11] H. Schweiger, P. Raybaud, H. Toulhoat, *J. Catal.* 212 (2002) 33.
- [12] J.V. Lauritsen, S. Helveg, E. Lægsgaard, I. Stensgaard, B.S. Clausen, H. Topsøe, F. Besenbacher, *J. Catal.* 197 (2001) 1.
- [13] P. Faye, E. Payen, D. Bougeard, *J. Catal.* 183 (1999) 396.
- [14] H. Schweiger, P. Raybaud, G. Kresse, H. Toulhoat, *J. Catal.* 207 (2002) 76.
- [15] B. Delley, *J. Chem. Phys.* 113 (2000) 7756.
- [16] A.D.J. Becke, *Chem. Phys.* 88 (1988) 2547.
- [17] J.P. Perdew, Y. Wang, *Phys. Rev. B* 45 (1992) 13244.
- [18] W. Kohn, L.J. Sham, *Phys. Rev. A* 140 (1965) 113.
- [19] P. Pulay, *J. Comp. Chem.* 3 (1982) 556.
- [20] B. Delley, in: J.M. Seminario, P. Politzer (Eds.), *Modern Density Functional Theory: A Tool for Chemistry: Theoretical and Computational Chemistry*, vol. 2, Elsevier Science, Amsterdam, 1995.
- [21] P. Raybaud, J. Hafner, G. Kresse, S. Kasztelan, H. Toulhoat, *J. Catal.* 189 (2000) 129.
- [22] S. Cristol, J.F. Paul, E. Payen, D. Bougeard, S. Clemendot, F. Hutshchka, *J. Phys. Chem. B* 104 (2000) 11220.
- [23] M.V. Bollinger, K.W. Jacobsen, J.K. Nørskov, *Phys. Rev. B* 67 (2003) 85410.
- [24] L.S. Byskov, B. Hammer, J.K. Nørskov, B.S. Clausen, H. Topsøe, *Catal. Lett.* 47 (1997) 177.
- [25] N. Nelson, R.B. Levy, *J. Catal.* 58 (1979) 485.
- [26] R.M. Laine, *Catal. Rev.-Sci. Eng.* 25 (1983) 459.
- [27] M. Zdrzil, *J. Catal.* 141 (1993) 316.
- [28] S. Rajagopal, R. Miranda, *J. Catal.* 141 (1993) 318.
- [29] Y. Zhao, P. Kukula, R. Prins, *J. Catal.* 221 (2004) 441.
- [30] F. Rota, V.S. Ranade, R. Prins, *J. Catal.* 200 (2001) 389.